Nonenantioselectivity Property of Human Deoxycytidine Kinase Explained by Structures of the Enzyme in Complex with L- and D-Nucleosides§

Elisabetta Sabini,† Saugata Hazra,† Manfred Konrad,‡ and Arnon Lavie*,†

Department of Biochemistry and Molecular Genetics, University of Illinois at Chicago, 900 S. Ashland Avenue, M/C 669, Chicago, Illinois 60607, and Max Planck Institute for Biophysical Chemistry, Am Fassberg 11, D-37077 Göttingen, Germany

Received January 8, 2007

Biological molecules are predominantly enantioselective. Yet currently two nucleoside analogue prodrugs (3TC and FTC) with opposite chirality compared to physiological nucleosides are clinically approved for the treatment of HIV infections. These prodrugs require conversion to their triphosphorylated forms to achieve pharmacological activity. The first step in the activation of these agents is catalyzed by human deoxycytidine kinase (dCK). This enzyme possesses the ability to phosphorylate nucleosides of the unnatural L-chirality. To understand the molecular basis for the nonenantioselectivity of dCK, we solved the crystal structures of the enzyme in complex with the L-enantiomer and of its physiological substrate deoxycytidine and with the L-nucleoside analogue FTC. These were compared to a structure solved with D-dC. Our results highlight structural adjustments imposed on the L-nucleosides and properties of the enzyme endowing it with the ability to phosphorylate substrates with nonphysiological chirality. This work reveals the molecular basis for the activation of L-nucleosides by dCK.

Introduction

Nucleoside analogues (NAs[a]) are a class of antiviral and anticancer prodrugs whose ability to mimic the structural and functional features of natural nucleosides allows them to interact with viral and/or cellular enzymes and to inhibit critical processes in the metabolism of nucleic acids. Among the drugs available for the treatment of human acquired immunodeficiency syndrome (AIDS), NAs play a major role targeting the viral RNA-dependent DNA polymerase, human immunodeficiency virus type-1 reverse transcriptase (HIV-1 RT). Currently, there are eight nucleoside analogue RT inhibitors that are approved by the U.S. Food and Drug Administration (FDA) for marketing in the U.S. Somewhat surprisingly, two of these eight NAs contain the L-chirality: 3TC ((2*R*,*cis*)-4-amino-1-[2-(hydroxymethyl)-1,3-oxathiolan-5yl]-(1*H*)-pyrimidin-2-one, also referred to as (−)-2′,3′-dideoxy-3′-thiacytidine, lamivudine) and FTC (5-fluoro-1-(2*R*,5*S*)-[2-(hydroxymethyl)-1,3-oxathiolan-5-yl]cytosine, emtricitabine), the latter being identical to 3TC except for the additional fluorine atom at position 5 of the cytosine base (Figure 1A).

In order to gain pharmacological activity, both L- and D-NAs require serial phosphorylation, via the mono- and the diphosphate intermediates, to the triphosphorylated form (NA-TP). This implies that, given their inverted configuration, the pharmacological activity of L-nucleoside analogues (L-NAs) is dependent on the capacity of all the enzymes of the activation pathway to phosphorylate enantiomers of opposite chirality, plus the ability of the L-NA-TP to successfully compete with physiological nucleoside triphosphates (NTPs) and to distinctively inhibit the viral (in the case of antiviral agents) or the cellular (in the case of anticancer agents) target DNA polymerases.

In human cells, the phosphorylation of nucleosides to the monophosphate form, which is often rate-limiting, is catalyzed by two cytosolic enzymes, thymidine kinase 1 (TK1) and deoxycytidine kinase (dCK), and by two mitochondrial enzymes, thymidine kinase 2 (TK2) and deoxyguanosine kinase (dGK). These four kinases have distinct, but overlapping, specificities. TK1 is specific for thymidine (dT), while dCK activates deoxycytidine (dC), deoxyadenosine (dA), and deoxyguanosine (dG). TK2 phosphorylates dT and dC, and dGK activates dA and dG.[1] These salvage pathway enzymes play a crucial role in supplying NTP precursors for DNA synthesis by phosphorylating the aforementioned physiological nucleosides, as well as in activating therapeutically relevant NAs.

Both of the L-nucleoside analogues 3TC and FTC are substrates of dCK, which converts them to the corresponding monophosphates. Further phosphorylation to the di- and triphosphates is accomplished by UMP/CMP kinase[2] and 3-phosphoglycerate kinase,[3] respectively. Both L-NA-TPs act as dCTP analogues, competitively inhibiting HIV reverse transcriptase and hepatitis B virus (HBV) DNA polymerase, and both can be incorporated into viral DNA causing chain termination.[4] In contrast to their D-enantiomers, 3TC and FTC are resistant to deamination by deoxycytidine deaminase (a strictly enantioselective enzyme[5,6]), a property that provides a clinical advantage for such molecules.[7]

A nucleoside, a nucleic acid base connected to a sugar moiety, has several chiral atoms. It is important to realize that all of the chiral centers of a nucleoside belong to the sugar moiety of the molecule (arrows, Figure 1A) rather than to its nucleic acid base. A cyclic form of the five-carbon sugar, as found in DNA and RNA, contains three or four chiral centers, respectively. It is

§ The following coordinates and structure factors have been deposited with the Protein Data Bank: C_4S·D-dC/ADP, 2NO1; C_4S·L-dC/ADP, 2NO7; C_4S·FTC/ADP, 2NO6.

* To whom correspondence should be addressed. Telephone: +1 312 355 5029. Facsimile: +1 312 355 4535. E-mail: Lavie@uic.edu.

† University of Illinois at Chicago.

‡ Max Planck Institute for Biophysical Chemistry.

[a] Abbreviations: NAs, nucleoside analogues; AIDS, acquired immunodeficiency syndrome; HIV-1 RT, human immunodeficiency virus type-1 reverse transcriptase; FDA, U.S. Food and Drug Administration; NA-TP, nucleoside analogue triphosphate; TK1, thymidine kinase 1; dCK, deoxycytidine kinase; TK2, thymidine kinase 2; dGK, deoxyguanosine kinase; dT, thymidine; dC, deoxycytidine; dA, deoxyadenosine; dG, deoxyguanosine; HBV, hepatitis B virus; BVdU, (*E*)-5-(2-bromovinyl)-2′-deoxyuridine; IdU, 5-iodo-2′-deoxyuridine; TRO, (−)-L-2′,3′-dideoxy-3′-oxacytidine (troxacitabine); AraC, cytarabine; C_4S-dCK, C9S/C45S/C59S/C146S dCK; ATP, adenosine triphosphate; ADP, adenosine diphosphate; UDP, uridine diphosphate; PDB, Protein Data Bank (http://www.rcsb.org).

10.1021/jm0700215 CCC: $37.00
Published on Web 05/27/2007

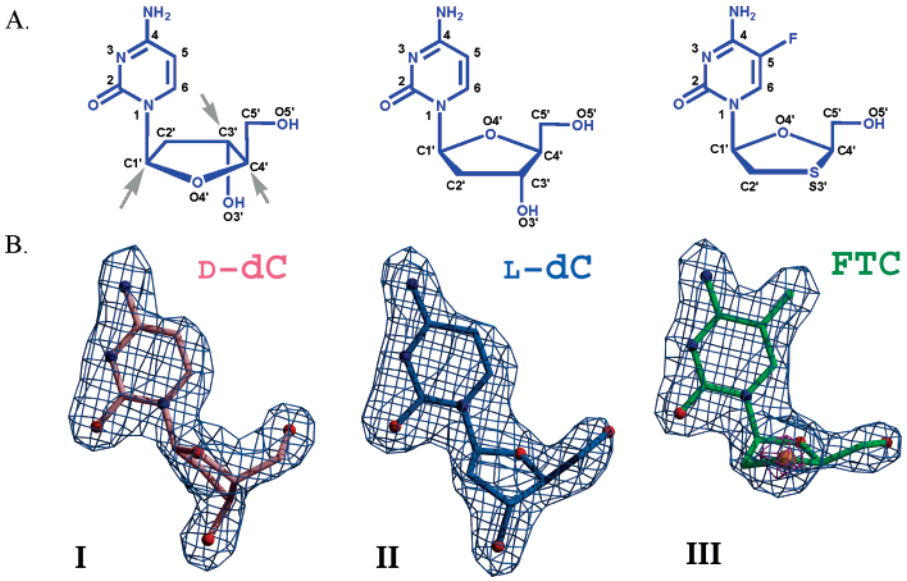

Figure 1. (A) Schematic representations of the structures of the D- and L-nucleosides presented in this paper. All are in the β-form: (I) D-dC, D-2′-deoxycytidine; (II) L-dC, L-2′-deoxycytidine, with L-dC being the mirror image (enantiomer) of D-dC; (III) FTC, (−)-L-β-2′,3′-deoxy-5-fluoro-3′-thiacytidine (emtricitabine). 3TC [(−)-L-β-2′,3′-dideoxy-3′-thiacytidine (lamivudine)] is similar to FTC, the only difference being the lack of the fluorine atom in position 5 of the cytosine ring. An additional L-NA mentioned in the text, TRO [(−)-L-2′,3′-dideoxy-3′-oxacytidine (troxacitabine)] differs from 3TC by having the sulfur atom in position 3′ of the ring replaced by an oxygen atom. (B) Experimental electron density map for the D- and L-nucleosides bound to the enzyme. D-dC is shown in pink, L-dC in blue, and FTC in green. The difference map ($F_{obs} - F_{calc}$) is contoured at 3σ (light blue). Note the strong signal given by the sulfur atom in FTC, still visible at 8σ (magenta).

the CH_2OH group at the C4 chiral center (ribose 4′ position) that determines if the nucleoside is designated D or L (Figure 1A). In addition, if the base connected via N1 to the sugar C1 atom (the glycosidic bond) is at the opposite side of the CH_2-OH group relative to the sugar ring, the sugar is referred to as the α-anomer. Conversely, if the base and the CH_2OH group are on the same side, the compound is a β-nucleoside. Physiological nucleosides are always of the β-D type. Whereas kinases display only residual activity on the α-anomers of the four possible permutations (α-D, β-D, α-L, and β-L), in some cases both β-forms are good substrates. The mirror symmetry relating the β-forms makes these molecules enantiomers. For simplicity we will omit the β-designation from the names of D- or L-nucleosides, but this configuration is implied unless noted otherwise.

It has been shown that the human nucleoside kinases dCK, dGK, and TK2 and the herpes simplex virus type 1 thymidine kinase (HSV-1 TK) are not enantioselective,[8] while human TK1 is strictly enantioselective and can only phosphorylate the natural D-form of thymidine.[9] Interestingly, dCK, dGK, and TK2 share high sequence similarity (dCK−dGK, 47% identity over 263 residues; dCK−TK2, 40% identity over 198 residues), and it has been suggested that HSV-1 TK evolved from a captured cellular dCK gene.[10] Structurally, these four enzymes belong to the same nucleoside kinase family[1] while TK1 makes a family of its own, as the determination of the three-dimensional structure of human TK1 has recently shown.[11] This points to a common feature present in dCK-like enzymes that confers relaxed enantioselectivity.

Human dCK presents relaxed enantioselectivity with respect to various pyrimidine and purine analogues, the enzyme favoring either the D- or the L-enantiomer depending on the substrate. For example, the L-nucleoside analogues 3TC and FTC (see Figure 1A) are good substrates of human dCK (Table S1 in Supporting Information). Remarkably, the L-enantiomers of both drugs are more efficiently phosphorylated by human dCK than the corresponding D-forms.[12] As a consequence, both 3TC and FTC show more potent antiviral activities than the corresponding D-enantiomer.[13] The anticancer L-NA troxacitabine (TRO, (−)-L-2′,3′-dideoxy-3′-oxacytidine) is also metabolized by dCK to its monophosphate.[14] Concerning purine nucleosides, it has been shown[15,16] that dCK accepts both D- and L-dA as substrates with similar efficiencies and with a slight preference for the unnatural L-enantiomer. Human dCK also displays a relaxed enantioselectivity with respect to dG, with only a 5-fold higher efficiency for D-dG compared to L-dG. Thus, the ability of dCK to phosphorylate both enantiomers is not limited to pyrimidine substrates. The low enantioselectivity of dCK concerns also the phosphate donor because it has been shown that the mouse enzyme accepts L-ATP and other L-nucleoside triphosphates with 15−30% of the activity of D-ATP.[17]

The nonenantioselective property of dCK is shared with the homologous dGK and TK2. While dGK favors the physiological D-enantiomer of dG, it phosphorylates L-dA more efficiently than D-dA and D-dG.[15,16] Mitochondrial TK2, in contrast with cytosolic TK1, shows a relaxed enantioselectivity, being able to recognize L-nucleosides such as L-dT, L-dC, L-BVdU ((*E*)-5-(2-bromovinyl)-2′-deoxyuridine), and L-IdU (5-iodo-2′-deoxyuridine).[18]

Previously we reported the structures of dCK in complex with the L-nucleoside analogues 3TC and TRO[19] and compared it to the complex with the D-enantiomer of dC. However, it was difficult to decouple the changes that are due to the difference in chirality from those that are due to the different nature of the sugar moiety: a 2′-deoxyribose sugar in the case of D-dC but a dioxolane or oxathiolane ring in the case of TRO and 3TC, respectively. To unambiguously understand how substrate chirality affects binding to the enzyme, structures of dCK in complex with the L- or D-form of the same nucleoside are needed. To this goal, we solved the three-dimensional structure of dCK in complex with L-dC and ADP. This allows us to directly compare the binding of the physiological substrate D-dC to its corresponding L-enantiomer. In addition, we report the structure of dCK in complex with the L-NA FTC. Comparison

Table 1. Data Collection and Refinement Statistics

	human dCK C9S/C45S/C59S/C146S (C_4S)		
	D-dC-ADP	L-dC-ADP	FTC-ADP
PDB code	2NO1	2NO7	2NO6
beamline	SERCAT BM-22	SERCAT BM-22	SERCAT BM-22
wavelength (Å)	1.0	1.0	1.0
temperature (K)	100	100	100
resolution (Å)	1.9 (1.9−2.0)	1.7 (1.7−1.8)	1.9 (1.9−2.0)
observed reflections	211763	399963	439005
unique reflections	42887	57715	43616
completeness (%)	98.6 (98.6)	94.4 (83.1)	99.3 (96.4)
R_{sym} (%)	10.8 (51.9)	7.8 (55.1)	8.7 (56.9)
$I/\sigma(I)$	10.6 (2.8)	15.3 (3.1)	16.7 (3.8)
space group	$C222_1$	$C222_1$	$C222_1$
unit cell			
a (Å)	52.7	52.8	52.8
b (Å)	132.8	133.4	134.3
c (Å)	156.8	156.0	155.0
molecules per au	2	2	2
refinement statistics			
R_{cryst} (%)	19.2	19.1	18.7
R_{free} (%)	24.1	24.3	23.4
resolution range (Å)	30−1.9	30−1.7	30−1.9
number of atoms			
protein	1984 (A)	2006 (A)	1995 (A)
	1854 (B)	1807 (B)	1845 (B)
nucleoside	16 × 2	16 × 2	16 × 2
ADP	27 × 2	27 × 2	27 × 2
water	192	289	178
rms deviation			
bond length (Å)	0.015	0.016	0.017
bond angle (deg)	1.632	1.780	1.723
average *B* factors (Å^2)			
protein	22 (A)	29 (A)	30 (A)
	24 (B)	29 (B)	33 (B)
main chain	21 (A)	28 (A)	29 (A)
	23 (B)	28 (B)	32 (B)
side chain	23 (A)	30 (A)	31 (A)
	24 (B)	31 (B)	34 (B)
ADP	16 (A)	22 (A)	22 (A)
	18 (B)	23 (B)	25 (B)
nucleoside	14 (A)	21 (A)	22 (A)
	14 (B)	22 (B)	28 (B)
waters	25	38	35
Ramachandran plot: non-glycine residues in			
most favored regions (%)	91.9	93.5	92.4
additionally allowed regions (%)	7.1	6.0	6.9
generously allowed regions (%)	1.0	0.5	0.7
disallowed regions (%)	0.0	0.0	0.0

of the FTC complex structure with that of the 3TC complex structure reveals the structural consequences of the ring fluorine atom (the sole atom differentiating FTC from 3TC).

Results

Generation of a Quadruple Cysteine Mutant To Improve Crystallization. Despite the essentiality of human dCK for the activation of numerous clinically relevant nucleoside analogues, structural information on how this enzyme recognizes a multitude of substrates has been hard to obtain because of difficulty in forming diffraction quality crystals. We rationalized that surface cysteines might hamper crystal growth. Of the six cysteine residues in dCK, we mutated the four surface-exposed ones to serines. The resulting C9S/C45S/C59S/C146S mutant, designated C_4S-dCK, in complex with L-nucleosides did actually crystallize much more easily than the wild type (WT) dCK. Interestingly, the C_4S-dCK crystals were obtained in the same precipitant used previously with the WT enzyme.[20] In order to verify that the mutations in C_4S-dCK did not perturb the structure, this protein was also crystallized in the presence of D-dC/ADP (see Figure 1 for the schematic structures of the nucleosides and the corresponding electron density maps) and compared to the same structures earlier solved in complexes with the WT enzyme.[20] Comparisons of the WT structures to the corresponding one solved with the C_4S mutant do not reveal any significant differences for either the main chain or the side chains of the protein or in the position of the substrates (Figure S1 of Supporting Information). The rmsd between WT-dCK·D-dC/ADP (PDB code 1P60) and C_4S·D-dC/ADP is 0.16 Å on 239 atoms. In addition, the C_4S mutant was kinetically characterized using ATP or UTP as phosphate donors and using D-dC, L-dC, FTC, and 3TC as acceptors (Table S1). Moderate kinetic differences (between 2- and 5-fold) in the catalytic efficiency were observed between the WT and the C_4S versions of dCK. These differences could be due to the four mutations inducing altered dynamic properties relative to the WT enzyme. In fact, we attribute the pronounced ability of the C_4S variant to crystallize to this change in the dynamic behavior of the enzyme. However, since we are dealing with static structures, this assumed difference in flexibility cannot be observed in the crystal structures. Nevertheless, the striking structural similarity of the two enzymes solved in complex with D-dC suggest that the C_4S mutant is an appropriate dCK variant from which we can obtain structural information relevant to WT dCK. In this

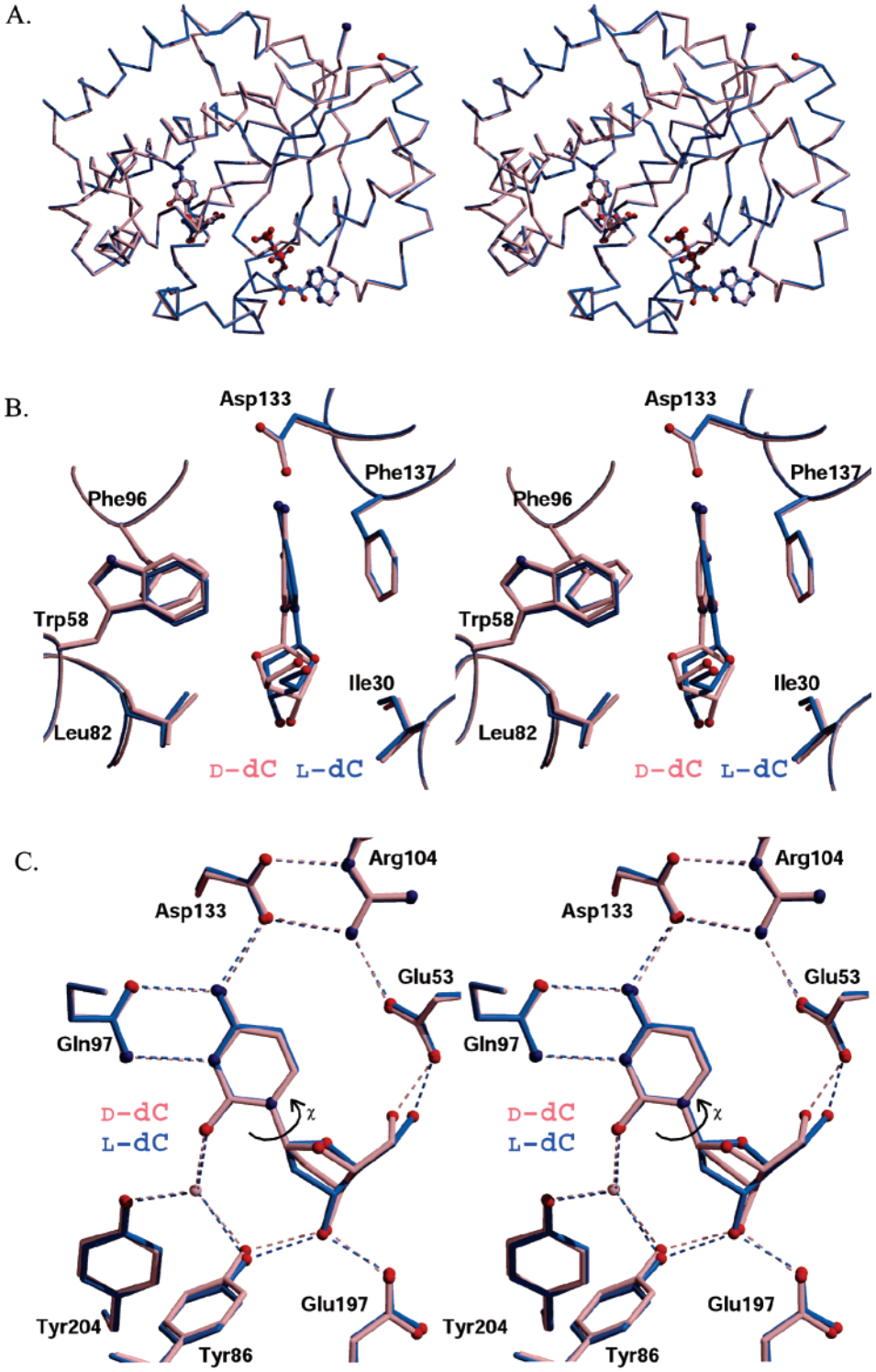

Figure 2. The conformation of dCK is preserved between structures solved in complex with D- or L-nucleosides. (A) Stereo representation of two superimposed structures of human dCK: the ternary complexes of the C_4S mutant with D-dC/ADP (pink), and L-dC/ADP (blue). The nucleosides D-dC and L-dC together with ADP are drawn using the same color scheme of the corresponding structures. (B and C) The position of active-site residues in the C_4S D-dC or L-dC complexes is very similar. (B) Hydrophobic interactions. Trp58, Phe96, and Phe137 create the hydrophobic pocket responsible for positioning of the cytosine base, while residues Leu82 and Ile30 create the hydrophobic environment responsible for positioning of the sugar moiety. Asp133 is drawn as reference. Note that the 3′-hydroxyl group of either D- or L-dC is positioned in a similar fashion by the enzyme. (C) Polar interactions. The "fingerprint" groups of the cytosine base ($-NH_2$, $-N-$, and $C{=}O$) maintain the same positions in the D- and L-molecules, preserving direct interactions with Gln97 and Asp133, and via a water molecule to Tyr86 and Tyr204. Water molecules and corresponding hydrogen bonds are drawn according to the same color scheme of the structures.

paper, when referring to structures of dCK, we imply the C_4S mutant unless otherwise stated.

Positioning of the Nucleoside Base in D- and L-Deoxycytidine Complexes. The goal of our work was to investigate how the enzyme manages to accommodate both D- and L-nucleosides in its active site. High-resolution diffracting crystals were obtained with ADP in the phosphoryl donor site and either the D-nucleoside D-dC or the L-nucleosides L-dC and FTC in the acceptor site (Table 1). The electron density difference maps for D-dC, L-dC, and FTC are shown in Figure

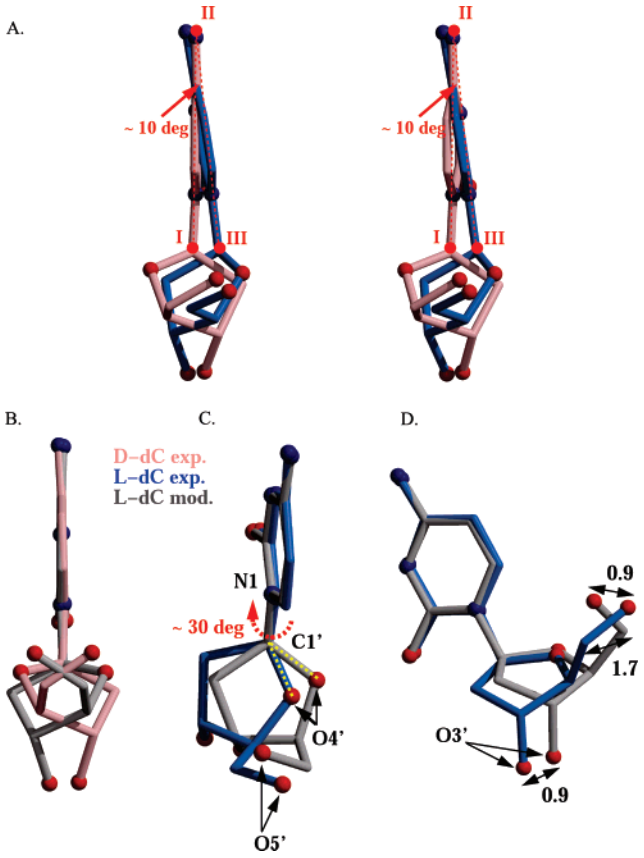

Figure 3. Changes in conformation between D- and L-dC bound to dCK. (A) L-dC (in blue), the enantiomeric form of the physiological substrate D-dC (pink), is accommodated by the dCK active site by tilting the position of its cytosine moiety by ~10°. In addition, there is a change in the glycosidic bond torsion angle and the exocyclic torsion angle is altered from gauche to trans (see also Table 3). Together, these adjustments position the 3′- and the 5′-hydroxyls in a similar fashion. (B) To quantify the change in the glycosidic bond torsion angle, we generated a model of L-dC (gray) that exactly corresponds to the mirror image of the experimentally observed D-dC (pink) molecule. (C) Overlay based on the atoms in the base of the modeled (gray) and the experimentally observed (blue) L-dC reveals a ~30° difference in the glycosidic torsion angle. (D) The distance of the 3′-hydroxyl group between the modeled and the experimental L-dC is 0.9 Å and that between the C5′ carbon is 1.7 Å. Note that because of the change in the exocyclic torsion angle, the overall position of the 5′-hydroxyl groups in the modeled versus the experimental L-dC is only 0.9 Å away.

Table 2. Glycosidic Bond Torsion Angle χ: O4′−C1′−N1−C2

	angle (deg)
D-dC	−132.0
L-dC, model	+132.0
L-dC, exptl	+162.0
3TC	+167.8
FTC	+168.3

1B. Comparison of D-dC to the L-dC structure shows that the overall fold of the protein is identical within coordinate errors (Figure 2A) with a rmsd between dCK•D-dC/ADP and dCK•L-dC/ADP being 0.18 Å on 239 atoms. In addition, the ADP molecules occupy the same position. The differences between the structures are limited to the conformation adopted by the L-dC versus the D-dC.

In both the D-dC and L-dC structures the cytosine base is in the anti conformation relative to the sugar moiety and it adopts a similar position. Binding of L-dC to the active site of dCK is similar to what we previously observed for the L-NAs 3TC and

Table 3. Exocyclic Torsion Angle γ: O5′−C5′−C4′ [C3′/S3′/O3′][a]

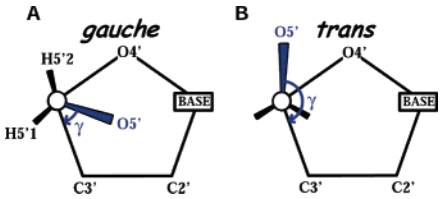

	angle (deg)
D-sugar: O5′ is gauche relative to C3′ and O4′	
D-dC	41.5
L-dC, model	−41.5
L-sugar: O5′ is trans relative to C3′/S3′ and gauche to O4′	
L-dC, exp.	−174.8
3TC	−171.2
FTC	−174.4

[a] Definition of the γ exocyclic torsion angle about the C4′−C5′ bond, looking in the direction of C5′ → C4′. Shown are schematics for D-nucleosides. (A) In this conformation, referred to as gauche, the O5′ atom is above the plane of the sugar ring and the γ angle can range from 30° to 90°. The O5′ atom is gauche with respect to both C3′ and O4′. This conformation, with a γ angle of ~45°, is observed for the D-nucleosides. (B) The conformation where the O5′ atom is trans to C3′ and gauche to O4′ is referred to in the text as trans. In this case the γ angle can range from 150° to 210°. L-Nucleosides adopt such a conformation. Because of the mirror relationship of L-nucleosides, the γ angle adopts a negative sign (about −170°). Note that an additional possible conformation (trans to O4′, gauche to C3′) is not depicted.

TRO.[19] Briefly, an aromatic pocket is created by residues Phe137, Phe96, and Trp58 (conserved within dCK, dGK, TK2, and HSV-1 TK): Phe137 stacks flat against the cytosine base, Phe96 approaches the center of the base at an angle, and finally, Trp58 is oriented perpendicular to the base (Figure 2B). In addition to these hydrophobic interactions, the polar atoms, which constitute the "fingerprints" of the cytosine base ($-NH_2$, −N−, and C═O), interact directly with active site residues (Figure 2C). Prominent among those is the conserved Gln97 that acts as hydrogen bond donor and acceptor toward the nitrogen and the amino group of the base, respectively. The cytosine amino group forms an additional hydrogen bond with Asp133. A further interaction made by the cytosine base of both the D- and the L-nucleosides presented here is through the carbonyl group. This group forms a hydrogen bond with Tyr204 and Tyr86 through bridging water molecules (Figure 2C). Tyr86 is conserved within dGK, TK2, and HSV-1 TK, while Tyr204 is conserved in dGK and TK2, but it is a methionine in HSV-1 TK. Note how the 3′-hydroxyl groups in D- and L-dC get positioned by the enzyme very close to each other and how consequently the interactions to residues Glu197 and Tyr86 are preserved in both structures (Figure 2C).

While the enzyme−nucleoside interactions are maintained regardless of enantiomer, the difference in chirality forces a slight change in position between the L- and D-dC. The cytosine base in the L-enantiomer tilts by ~10° relative to its position as observed with the D-enantiomer (Figure 3A) while maintaining the "fingerprint" groups of the cytosine base nearly in the same positions between the D- and L-molecule. These polar atoms are in fact most important for the recognition and stabilization of the cytosine base through interactions with residues Gln97, Asp133, and Tyr204/Tyr86 via water molecules, as previously described.

Positioning of the Sugar Ring in D- and L-Deoxycytidine Complexes. A further difference between the binding modes of L-dC and D-dC is manifested in the orientation of the sugar ring relative to the base (i.e., the glycosidic bond torsion angle,

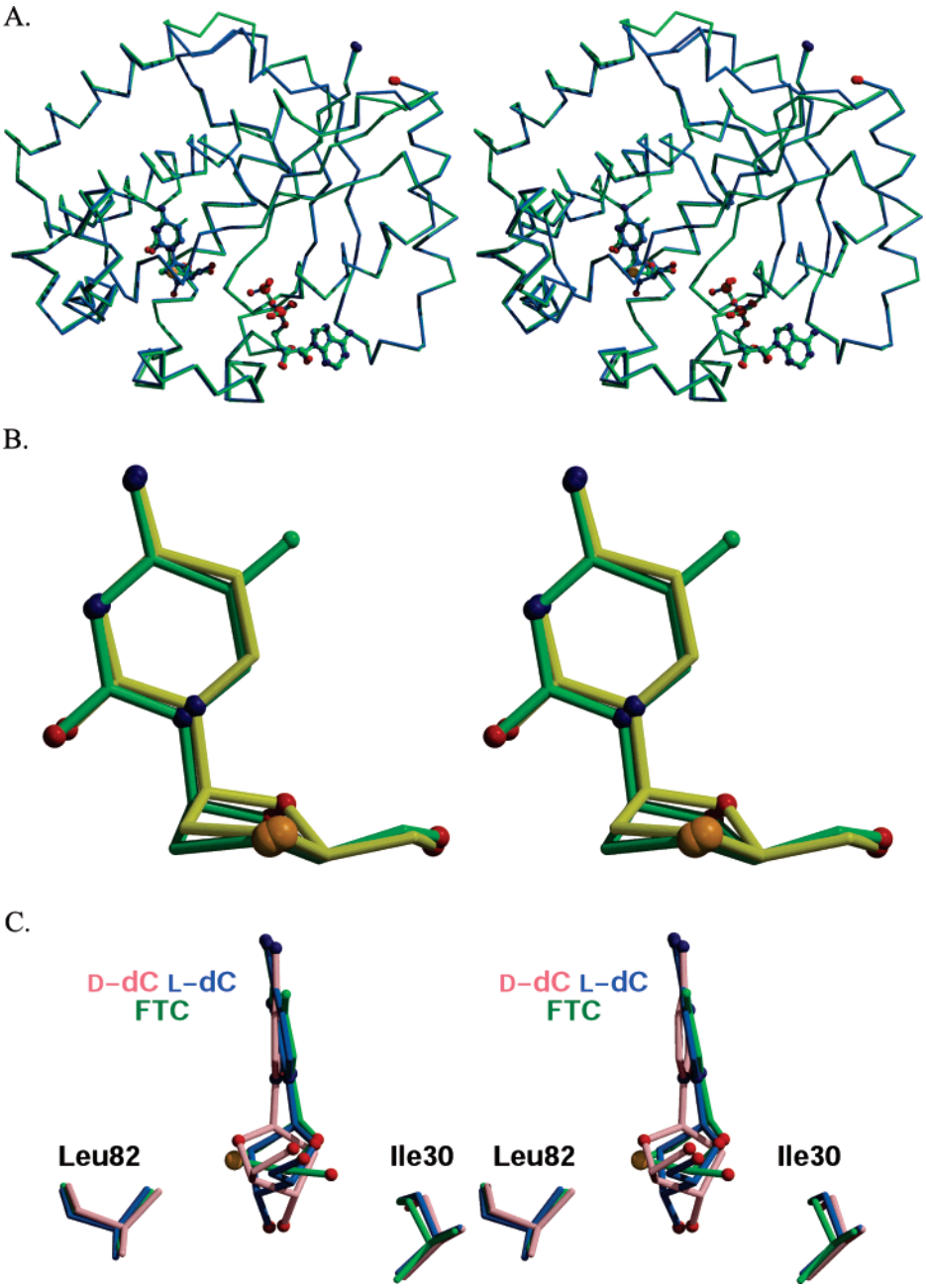

Figure 4. (A) Stereo representation of the overlay of the structures of C_4S·L-dC/ADP (blue) to the one of C_4S·FTC/ADP (green) showing the strict similarity between the two. This is also true for the overall fold of 3TC and TRO when compared to the one of L-dC (not shown). (B) Zooming in of the active site of dCK showing the similar binding of FTC (green) and 3TC (yellow). (C) Stereo representation of the comparison of FTC (green) to D-dC (pink) and L-dC (blue). Given the fact that the positions of the enzyme's active site residues do not change appreciably between the D- and the L-nucleosides, the nucleosides have to bind while maintaining a similar position for (i) the cytosine base, (ii) the 5′-hydroxyl group, and (iii) the 3′-hydroxyl group. This is achieved by tilting the cytosine base in the L- versus the D-nucleosides and by changing both the glycosidic and the exocyclic torsion angles. Residues Leu82 and Ile30 confine the sugar ring in a catalytically competent conformation.

Table 2). To quantify the difference in glycosidic torsion angles between D-dC and L-dC, we generated a theoretical model of the L-form of dC (in gray, Figure 3B) that is the exact mirror image of the D-dC molecule as observed in our structure (in pink, Figure 3B). We then overlaid the base moieties of this modeled L-dC and the experimentally observed L-dC and measured the difference in the glycosidic bond torsion angles (Figure 3C,D). This revealed that the sugar in L-dC upon binding to dCK rotates about 30° around the glycosidic bond relative to the conformation adopted by D-dC when bound to the enzyme (Figure 3C, red arrow). The possible glycosidic bond torsion angles are limited in the active site of dCK by the hydrophobic residues Ile30 and Leu82 (Figure 2B). Our modeling also revealed that the sugar pucker between L- and D-dC is basically unchanged (C3′ exo). In contrast, the O5′-hydroxyl, the moiety that accepts the phosphoryl group from ATP, adopts a ∼130° different conformation in the L-dC versus the D-dC structure (Figure 3C,D). This difference in position of the O5′ atom with respect to O4′ and C3′ atoms changes the torsion angle about the C4′ and C5′ bond from gauche in the D-dC structure to trans in the L-dC structure (Table 3).

In summary for this section, our results demonstrate that upon binding of the L-enantiomeric form of dC to dCK, three significant changes occur: (1) the relative tilting of the base by 10°, (2) the relative rotation around the glycosidic bond by 30°, and (3) the change in the exocyclic torsion angle by 130°.

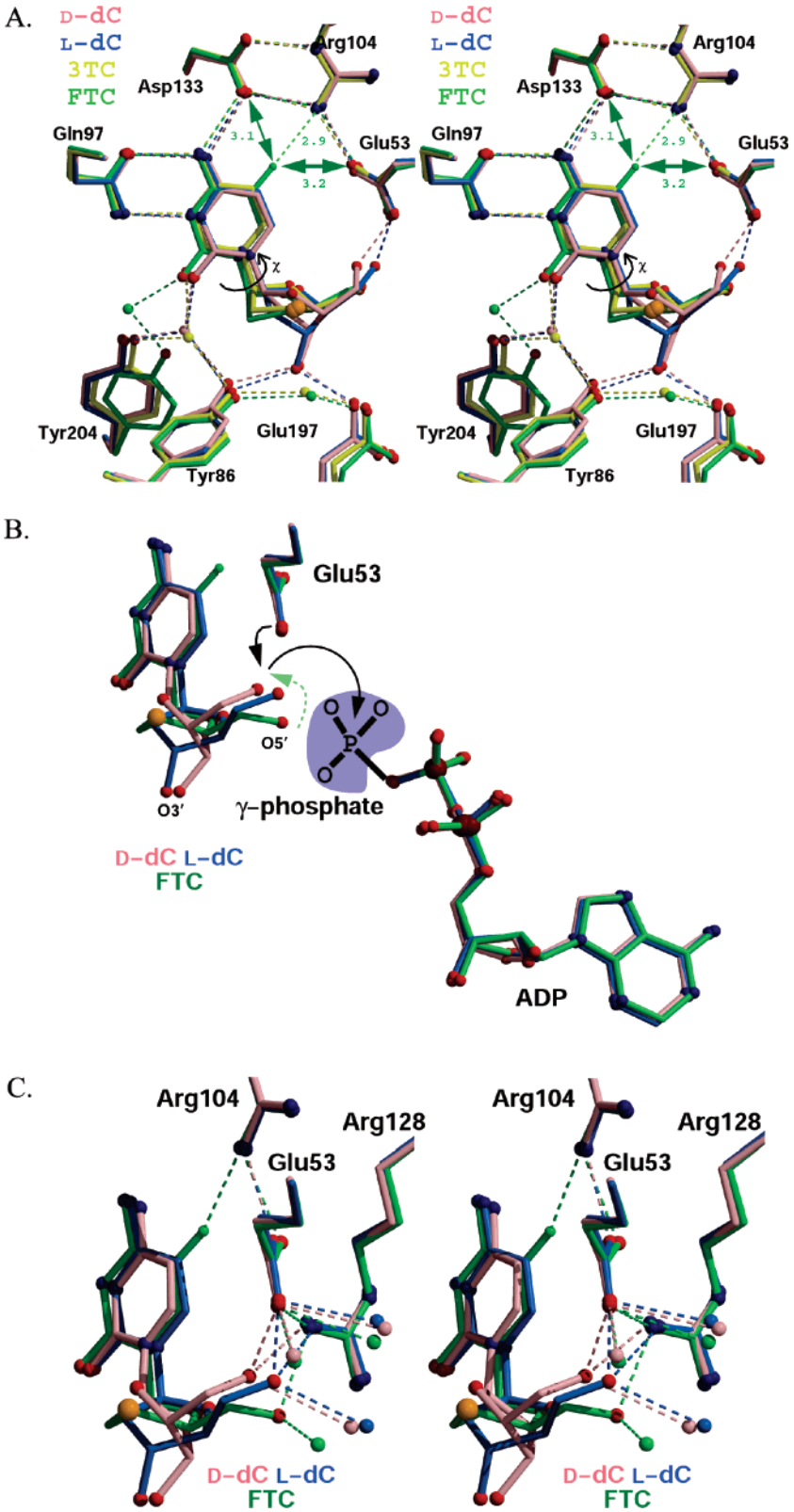

Figure 5. (A) Comparison of the binding of FTC (green) and 3TC (yellow) to the binding of L-dC (blue) and D-dC (pink) in the active site of dCK. The positions of the active site residues of dCK in the four structures are very similar. The only slight difference is observed in the rotation of Tyr204 in FTC and in the movement of Glu197 in both the FTC and 3TC structures. Because of the two close interactions of the fluorine atom in FTC to Asp133 and Glu53, the entire FTC molecule slightly translates toward Gln97, thus displacing the water molecule bridging the base to Tyr204 and Tyr86 in the other structures. Consequently, Tyr204 in the FTC complex adopts a different conformation relative to the other complexes. The slight deviation in the position of Glu197 in the FTC and 3TC complex structures is probably due to the lack of a 3′-hydroxyl group in these two L-NAs. As a result, a water molecule mimics the absent 3′-hydroxyl and recapitulates its function by bridging Glu197 and Tyr86. (B) Overlay of the nucleosides/nucleotides present in the three structures. Glu53 acts to deprotonate the nucleoside 5′-OH group, which proceeds to attack the ATP γ-phosphate (black arrows). The γ-phosphate is depicted schematically in a purple background. Note the nearly identical overlay of the ADP molecules. In contrast, the L-nucleosides adjust their conformation as discussed in the text. In order for the 5′-OH of FTC to interact with Glu53, a rotation around the C4′−C5′ bond is required (green dashed arrow). (C) The 5′-hydroxyl groups in D-dC and L-dC directly interact with both Glu53 and Arg128, while the 5′-OH of FTC directly interacts with Arg128 only.

It is the compulsory combination of these three changes that positions the 3′- and 5′-hydroxyl groups at a very similar manner irrespective of the enantiomeric nature of dC. On the basis of this similarity in positioning of the 5′-hydroxyl, one could have predicted that L-dC would be a good substrate of dCK. This is indeed the case, albeit with a 3- to 5-fold lower k_{cat} in comparison to D-dC. Given the static nature of crystal structures, it is hard to identify a clear explanation for the subtle decrease in catalytic rate for the L-form of dC.

Binding Characteristics of the Prodrug FTC. To gain insight into the mode of binding of medicinally relevant L-NAs, we solved the structure of dCK in complex with FTC at the phosphoryl acceptor site and with ADP at the donor site (Table 1). Superposition of the structures of L-dC/ADP and FTC/ADP shows that the overall fold of the protein (Figure 4A) and the position of the active site residues are identical within coordinate errors, with a rmsd between dCK·L-dC/ADP and dCK·FTC/ADP being 0.29 Å on 240 atoms. Moreover, overlay of the FTC structure on the structures of dCK in complex with the nucleoside analogue 3TC[19] shows that the two L-NAs maintain a similar positioning of the base and of the sugar (Figure 4B) with comparable exocyclic (trans) and glycosidic torsion angles (Tables 2 and 3).

Upon binding in the dCK active site, FTC shows the same 10° tilting of the base relative to D-dC as previously described for L-dC (Figure 3A). This suggests that accommodation of L-nucleosides by base tilting relative to D-nucleosides is a general feature of dCK, regardless of the nature of the sugar moiety. This phenomenon is shown in more detail in Figure 4C where the binding of FTC (green) is compared to the one of D-dC (pink) and L-dC (blue). Concerning the sugar pucker for the three molecules, it is C3′ endo in FTC and C3′ exo in D- and L-dC. This difference in sugar pucker can be attributed to a lack of a 3′-hydroxyl group in FTC or to an intrinsic property of the oxathiolane moiety of FTC.

Despite the similarity in the tilting of the base among the L-nucleosides, both FTC and 3TC bind to the active site of dCK in a slightly different way compared to L-dC. Both oxathiolane containing L-NAs, in comparison to L-dC, are positioned somewhat deeper in the active site (∼0.5 Å), with a concomitant adjustment of the side chain of Gln97 (Figure 5A). This different position can be attributed to lack of the 3′-hydroxyl group in the two prodrugs, resulting in loss of the positioning interaction with residues Tyr86 and Glu197. In the FTC and 3TC complex structures, a water molecule is observed to mimic the missing 3′-hydroxyl group, reestablishing a bridging function between Tyr86 and Glu197. Whereas this feature is common to both the FTC and 3TC structures, the fluorine atom at position 5 of the cytosine base in FTC (green) causes an additional adjustment of this nucleoside. The fluorine atom makes a 2.9 Å hydrogen bond with the imido group of Arg104, but it is also subjected to two repulsive interactions with residues Asp133 and Glu53 (at 3.1 and 3.2 Å, respectively). As a consequence, the cytosine base in FTC is positioned slightly lower than 3TC, resulting in a displacement of the water seen in the other complexes to bridge the carbonyl group of the base with residues Tyr204 and Tyr86 (Figure 5A). To compensate for the loss of this water, the Tyr204 side chain in FTC complex rotates placing its hydroxyl group near to the position of the displaced water molecule.

The position and the interactions involving the 5′-hydroxyl group (the hydroxyl group that takes part in the chemical reaction) of the prodrug FTC are different when compared to the positions and interactions of L-dC and D-dC. For both enantiomers of dC, the O5′-hydroxyl is located at a catalytically active distance (2.5 and 2.4 Å in D-dC and L-dC, respectively) to Glu53, the general base that activates the sugar 5′-OH to attack the γ phosphate of ATP (Figure 5B). Despite the opposite chirality of the two molecules, proper positioning is maintained through a change in the exocyclic torsion angle in L-dC relative to the one in D-dC (Table 3), as previously discussed. In contrast, in FTC, the 5′-hydroxyl group is located 1.4 Å from the corresponding 5′-hydroxyl groups of D-dC and L-dC (Figure 5C). As a result, the distance between Glu53 and the 5′-OH in FTC increases to 3.4 Å. At the same time, modeling a rotation around the C5′−O5′ bond demonstrates that the 5′-OH atom in FTC can easily form the catalytically critical interaction with the carboxylic moiety of Glu53. However, given the sugar pucker (C3′ endo) observed for FTC, this rotation is disfavored because it would not be possible to concomitantly maintain ideal distances to Glu53 and Arg128, as is the case of L- and D-dC. However, the fact that dCK shows catalytic efficiency toward FTC (lacking the direct O5′-Glu53 interaction) similar to that of L-dC (making a direct O5′−Glu53 interaction) (Table S1) suggests that the nonoptimal conformation observed for O5′ in the FTC structure does not affect the rate-limiting step of the phosphoryl transfer reaction.

In summary, the key points in the binding of the D- and the L-nucleosides are the stabilization of the cytosine base within the aromatic pocket and through interactions with Gln97 and Asp133, and the positioning of the 5′-hydroxyl group so that it can directly (D-dC, L-dC) or after a slight rotation (FTC) make a catalytically active interaction with Glu53. These goals can be achieved regardless of whether the substrate is an L- or D-nucleoside by allowing the base to adopt a different position, by changing the sugar orientation in order to minimize steric hindrances with residues Ile30 and Leu82, and finally, by rotation of the 5′-OH around the C5′−O5′ bond.

Discussion

Enantioselectivity is an evolution-driven ability of enzymes to selectively recognize and metabolize the physiological enantiomer of chiral substrates. This property has even been exploited for the chemical synthesis of nucleoside analogues. For example, the strictly enantioselective cytidine deaminase has been used to exclusively deaminate (+)-2′-deoxy-3′-thiacytidine (BCH-189) from the racemic mixture (±)-BCH-189, thus selectively sparing the L-enantiomer (−)-BCH-189, also known as 3TC.[21] However, a small number of enzymes show a relaxed enantioselectivity toward their substrates. This is true for the deoxynucleoside kinase dCK and homologous family members dGK, TK2, and HSV-1 TK. These are key enzymes in the activation process of nucleoside analogues used to treat viral infections and cancer. Still, the relaxed enantioselectivity of these enzymes has not been fully exploited toward the development of improved approaches to antiviral or anticancer chemotherapy. To understand what molecular factors endow such nonenantioselectivity, we solved the crystal structure of dCK in complex with β-D- and β-L-nucleosides.

The interaction between dCK and its nucleoside substrates is predominately mediated via the base moiety. Hydrophobic interactions sandwich the base, while its polar atoms make interactions with polar and charged side chains of the enzyme. In contrast, the sugar makes only a few interactions with the enzyme, and here, the critical aspect is the correct positioning of the 5′-OH, the group that becomes phosphorylated during the reaction. Therefore, it is the base part of the nucleoside that determines how the molecule will bind in the active site. But it

is ultimately the positioning of the 5′-OH that will determine if a certain nucleoside will be phosphorylated or not.

This being the case, when it comes to the four diastereomeric variants of the natural substrate of dCK (α or β D-dC, α or β L-dC), it is not surprising that the α anomers are not, or at most very poor, substrates.[22] In the α form, the 5′-OH is on the opposite side of the sugar ring relative to the cytosine base. As a result, the 5′-OH group is too far from an invariable carboxylic acid side chain (Glu53 in human dCK) whose role is to increase the nucleophilicity of the 5′-OH (Figure 5B). In contrast, our structures reveal that for either the D- or L- β-anomer, the binding mode of the base is compatible with the correct positioning of the 5′-OH for catalysis to take place.

However, because of the spatial differences between enantiomeric L- and D-nucleosides, productive binding of the β-L-substrates to dCK necessitates conformational changes of L-nucleosides relative to D-nucleosides. These conformational adjustments are seen in (i) the tilting of the base, (ii) the rotation of the sugar around the glycosidic bond, and (iii) the rotation of the O5′-hydroxyl group. A change in sugar pucker also exists between deoxyribose containing nucleosides (e.g., D-dC and L-dC) and analogues that contain a modified sugar (e.g., FTC). However, this difference is probably unrelated to the difference in chirality but rather is due to the differences within the sugar moiety. Common to all L-nucleosides is a tilting of the base by approximately 10° in comparison to its position taken upon β-D-nucleoside binding (Figures 3A and 4C). This tilting of the base is driven by the need to avoid a clash between the sugar moiety and Leu82, which is on the opposite side of the active site residue Ile30 (Figures 2B and 4C). Importantly, despite this base tilting, the interactions between the enzyme and the "fingerprint" atoms of the dC base (that is, the N and O atoms of the ring) are maintained. While the positions of these atoms are unchanged within coordinate error between the structures of L- and D- nucleosides, the glycosidic N-atom is shifted 0.5−0.6 Å toward Phe137 in the case of L-nucleosides (Figure 2B).

The consequence of this base slanting is a 0.8−1.0 Å shift toward Ile30 of the C1′ glycosidic carbon relative to its position in D-nucleosides (Figures 2B and 4C). Modeling in the active site of dCK of an L-dC molecule having the same glycosidic bond torsion angle of D-dC (L-dC modeled in gray, Figure 3B−D) shows that if only this base shift were to occur, then the sugar would still be too close to Ile30 and Arg128. Thus, an additional rotation around the glycosidic bond is required to avoid a repulsive interaction. This change in the glycosidic bond torsion angle corresponds to a difference of approximately 30° between the L- and D-nucleosides (see Table 2).

We conclude that the ability of dCK to phosphorylate the β-form of enantiomeric nucleosides is due to both the nature of the enzyme's active site and the nature of the substrates. The major attribute of the enzyme is that most of the binding interactions between substrate and enzyme are directed at the base moiety of the nucleoside. If, however, upon binding of L-nucleosides, the enzyme mandated an invariant orientation of the sugar ring compared to the one of D-nucleosides, then the base moiety would be forced to point in the opposite direction. Such a scenario is not tolerated by the dCK active site. Therefore, in dCK it is the base that dictates the binding, requiring a similar orientation of this moiety in L- and D-substrates, and it is the sugar that is forced to change its orientation. More specifically, the interactions with the higher degree of space constraints are those made between the base's polar atoms and the enzyme's active site side chains. Once these are made, the slightly different structure of an L-nucleoside requires only a small tilt of the base and a change in the glycosidic bond torsion angle to fit in the tolerant dCK active site.

A reason for this active site plasticity could be the physiological role of this enzyme to phosphorylate both the pyrimidine dC and the purines dA and dG. Indeed, overlay of our structures solved with pyrimidines[20] to that solved with a purine analogue[23] shows that the side chains of Gln97 and Asp133 shift slightly deeper into the active site when the larger purine is bound and that the sugar moiety is somewhat differently positioned in comparison to dC. Thus, substrate-positioning flexibility is an inherent property of the dCK active site that allows for the correct orientation of the sugar 5′-OH for activation by Glu53 no matter if the nucleoside is a purine or a pyrimidine. An additional consequence of this plasticity is the lack of enantioselectivity by dCK.

In fact, the other human nucleoside kinases that are non-enantioselective, dGK and TK2, must also phosphorylate more than a single substrate. Thus, the requirement to accommodate dA and dG by dGK and to accommodate dT and dC by TK2 could also serve to explain their lack of enantioselectivity. Likewise, the ability of HSV-1 TK to phosphorylate L-nucleosides can be correlated with the ability of this enzyme to phosphorylate different substrates, such as dT, dTMP, and the guanosine analogues acyclovir and ganciclovir. In contrast, human TK1, whose role is limited to dT phosphorylation, is indeed an enantioselective enzyme. The conclusion here is that enzymes that have evolved to accept several different substrates acquired a structurally less restricted active site, which in turn can endow these enzymes with unexpected activities on enantiomeric substrates.

While the unique nature of the enzyme's active site plays an important role in permitting productive binding of L-nucleosides, the nature of the nucleoside substrate itself is also a part of the story. The base lacks chiral atoms and thus plays no role here, and all the differences between L- and D-enantiomers are due to the relative orientations of substituents present in the sugar ring. As mentioned before, of the four forms of dC, it is only the two sugar β-configurations that are catalytically competent because the enzyme requires that the base and the CH_2OH groups point to the same side of the sugar ring. So the question reduces to the following: What makes β-L and β-D nucleosides special that both can act as substrates? The symmetry operation that relates D- and L- nucleosides is the mirror operation. In most cases objects that have mirror symmetry cannot be overlaid well, just as the left-hand cannot be overlaid on the right-hand. However, in the case of L- and D- nucleosides, because of the position where the CH_2OH substituent is connected to the sugar ring, i.e., the C4′ atom, the mirror relationship still allows for a nearly perfect overlay of the critical O5′ atom. A slight tilting of the base, concomitant with a change in the glycosidic bond torsion angle and allowed by the permissive dCK active site, combined with a rotation of the O5′-hydroxyl is all that is needed for phosphoryl transfer to take place. In other words, the special character of nucleosides that have the differentiating chiral atoms lying close to a pseudomirror plane running through the base (atom C1′ and midway the bond between C3′ and C4′) results in molecules that can be overlaid well, bringing the critical C5′ atom within 1 Å between each other. This allows dCK to position L- and D-nucleosides in a congruent fashion.

Our work demonstrates how two factors, the promiscuity of the enzymes in question and the special nature of their substrates, allow phosphorylation of nucleosides with opposing chirality to their physiological substrates. As a consequence of this

relaxed enantioselectivity of dCK and the related dGK and TK2, the field of L-nucleosides holds promise for the development of efficient and selective drugs against cancer and viral infections.

Experimental Section

Site-Directed Mutagenesis, Protein Expression, Purification, and Crystallization. The dCK mutant C9S/C45S/C59S/C146S (C_4S-dCK) was created using the QuickChange Site-Directed mutagenesis kit from Stratagene, using as template the wild type dCK gene cloned into the pET14b vector, as previously described.[19] For protein expression, the BL21(DE3) *Escherichia coli* strain carrying the recombinant plasmid coding for His-tagged C_4S-dCK was grown in 2YT media at 37 °C, induced with 0.1 mM IPTG and harvested after 4 h. The cell pellet was lysed by sonication and loaded onto a HisTrap HP column packed with 5 mL of Ni Sepharose high-performance resin (Amersham Biosciences). After loading, the column was washed with 500 mL of buffer containing 20 mM imidazole, pH 7.5, and protein was eluted with 200 mM imidazole (in 50 mM HEPES, pH 7.5, and 500 mM NaCl). EDTA (2 mM) was immediately added to the eluted protein to avoid degradation by traces of proteases. The His-tag was not cleaved, and the protein was further purified on an S-200 gel filtration column (Amersham Biosciences) using as gel filtration buffer 20 mM Hepes, pH 7.5, 200 mM sodium citrate, and 2 mM EDTA. The C_4S mutant was then crystallized in complex with ADP and the nucleoside D-dC, L-dC, or FTC using the vapor diffusion method in the hanging-drop geometry. The D-nucleosides and the nucleotides were purchased from Sigma, while FTC was obtained through the NIH AIDS Research and Reference Reagent Program, Division of AIDS. After the respective complexes were formed by mixing of the nucleoside or nucleoside analogue and ADP (final concentrations of 5 mM each) and enzyme (10−20 mg/mL of C_4S-dCK in gel filtration buffer plus 5 mM $MgCl_2$), 1 μL of the premixed solution was added to 1 μL of the reservoir solution and left to equilibrate at 20 °C against the reservoir. Orthorhombic crystals were obtained from hanging drops using a reservoir solution that contained 0.95−1.5 M trisodium citrate dihydrate and 100 mM HEPES, pH 7.5.

Data Collection and Processing. Crystals were transferred to a cryoprotectant solution consisting of mineral oil (Sigma), mounted in loops, and frozen by directly immersing them in liquid nitrogen. X-ray data were collected at the Advanced Photon Source using the SERCAT beamline BM-22. The data were indexed, scaled, and merged using XDS and XSCALE[24] (see Table 1 for data collection statistics).

Structure Determination and Refinement. The original structure of the C_4S mutant[19] was solved by molecular replacement (MOLREP[25]) using the wild type dCK·D-dC·ADP structure (PDB code 1P60[20]) as search model. The four structures presented here required only rigid body refinement of the original C_4S structure because of crystallization in the same space group. Refinement was carried out using REFMAC,[26] and simulated annealing maps were calculated using CNS.[27] Rebuilding was done in O[28]. The nucleoside and the nucleotide molecules were modeled into the electron density maps (Figure 1B) after most of the protein and the water atoms were built and refined.

Steady-State Kinetic Assay. A spectroscopic enzyme-coupled assay was used to determine enzyme activity as described previously[29] in 50 mM Tris-HCl, pH 7.5, 100 mM KCl, and 5 mM $MgCl_2$ at 37 °C with 0.35 μM dCK, 1 mM ATP-Mg, and 1 mM UTP-Mg. Nucleoside/nucleoside analogue concentrations were varied between 5 and 100 μM.

Acknowledgment. We thank Dr. Stephen K. Burley for useful discussions and the staff at the SER-CAT beamline for help in data collection. We acknowledge Dr. Gilles Gosselin for providing a sample of L-dC. FTC was obtained through the AIDS Research and Reference Reagent Program, Division of AIDS, NIAID, NIH. This work was supported by an NIH grant (E.S., S.H., and A.L.) and the Max-Planck-Society (M.K.)

Supporting Information Available: Stereo representations of WT-dCK and C_4S variant in complex with D-dC and ADP and table of kinetic data for WT and C_4S-dCK. This material is available free of charge via the Internet at http://pubs.acs.org.

References

(1) Eriksson, S.; Munch-Petersen, B.; Johansson, K.; Eklund, H. Structure and function of cellular deoxyribonucleoside kinases. *Cell. Mol. Life Sci.* **2002**, *59*, 1327−1346.
(2) Pasti, C.; Gallois-Montbrun, S.; Munier-Lehmann, H.; Veron, M.; Gilles, A. M.; Deville-Bonne, D. Reaction of human UMP-CMP kinase with natural and analog substrates. *Eur. J. Biochem.* **2003**, *270*, 1784−1790.
(3) Krishnan, P.; Gullen, E. A.; Lam, W.; Dutschman, G. E.; Grill, S. P.; Cheng, Y. C. Novel role of 3-phosphoglycerate kinase, a glycolytic enzyme, in the activation of L-nucleoside analogs, a new class of anticancer and antiviral agents. *J. Biol. Chem.* **2003**, *278*, 36726−36732.
(4) Feng, J. Y.; Anderson, K. S. Mechanistic studies examining the efficiency and fidelity of DNA synthesis by the 3TC-resistant mutant (184V) of HIV-1 reverse transcriptase. *Biochemistry* **1999**, *38*, 9440−9448.
(5) Shafiee, M.; Griffon, J. F.; Gosselin, G.; Cambi, A.; Vincenzetti, S.; Vita, A.; Eriksson, S.; Imbach, J. L.; Maury, G. A comparison of the enantioselectivities of human deoxycytidine kinase and human cytidine deaminase. *Biochem. Pharmacol.* **1998**, *56*, 1237−1242.
(6) Chang, C. N.; Doong, S. L.; Zhou, J. H.; Beach, J. W.; Jeong, L. S.; Chu, C. K.; Tsai, C. H.; Cheng, Y. C.; Liotta, D.; Schinazi, R. Deoxycytidine deaminase-resistant stereoisomer is the active form of (+/−)-2′,3′-dideoxy-3′-thiacytidine in the inhibition of hepatitis B virus replication. *J. Biol. Chem.* **1992**, *267*, 13938−13942.
(7) Verri, A.; Focher, F.; Priori, G.; Gosselin, G.; Imbach, J. L.; Capobianco, M.; Garbesi, A.; Spadari, S. Lack of enantiospecificity of human 2′-deoxycytidine kinase: relevance for the activation of beta-L-deoxycytidine analogs as antineoplastic and antiviral agents. *Mol. Pharmacol.* **1997**, *51*, 132−138.
(8) Maury, G. The enantioselectivity of enzymes involved in current antiviral therapy using nucleoside analogues: a new strategy? *Antiviral Chem. Chemother.* **2000**, *11*, 165−189.
(9) Wang, J.; Chattopadhyaya, J.; Eriksson, S. The enantioselectivity of the cellular deoxynucleoside kinases. *Nucleosides Nucleotides* **1999**, *18*, 807−810.
(10) Harrison, P. T.; Thompson, R.; Davison, A. J. Evolution of herpesvirus thymidine kinase from cellular deoxycytidine kinase. *J. Gen. Virol.* **1991**, *72*, 2583−2586.
(11) Welin, M.; Kosinska, U.; Mikkelsen, N. E.; Carnrot, C.; Zhu, C.; Wang, L.; Eriksson, S.; Munch-Petersen, B.; Eklund, H. Structures of thymidine kinase 1 of human and mycoplasmic origin. *Proc. Natl. Acad. Sci. U.S.A.* **2004**, *101*, 17970−17975.
(12) Shewach, D. S.; Liotta, D. C.; Schinazi, R. F. Affinity of the antiviral enantiomers of oxathiolane cytosine nucleosides for human 2′-deoxycytidine kinase. *Biochem. Pharmacol.* **1993**, *45*, 1540−1543.
(13) Gumina, G.; Chong, Y.; Choo, H.; Song, G.-Y.; Chu, C. L-Nucleosides: antiviral activity and molecular mechanism. *Curr. Top. Med. Chem.* **2002**, *2*, 1065−1086.
(14) Weitman, S.; Marty, J.; Jolivet, J.; Locas, C.; Von Hoff, D. D. The new dioxolane, (−)-2′-deoxy-3′-oxacytidine (BCH-4556, troxacitabine), has activity against pancreatic human tumor xenografts. *Clin. Cancer Res.* **2000**, *6*, 1574−1578.
(15) Gaubert, G.; Gosselin, G.; Boudou, V.; Imbach, J. L.; Eriksson, S.; Maury, G. Low enantioselectivities of human deoxycytidine kinase and human deoxyguanosine kinase with respect to 2′-deoxyadenosine, 2′-deoxyguanosine and their analogs. *Biochimie* **1999**, *81*, 1041−1047.
(16) Gaubert, G.; Gosselin, G.; Imbach, J. L.; Eriksson, S.; Maury, G. Derivatives of L-adenosine and L-guanosine as substrates for human deoxycytidine kinase. *Nucleosides Nucleotides* **1999**, *18*, 857−860.
(17) Tomikawa, A.; Kohgo, S.; Ikezawa, H.; Iwanami, N.; Shudo, K.; Kawaguchi, T.; Saneyoshi, M.; Yamaguchi, T. Chiral discrimination of 2′-deoxy-L-cytidine and L-nucleotides by mouse deoxycytidine kinase: low stereospecificities for substrates and effectors. *Biochem. Biophys. Res. Commun.* **1997**, *239*, 329−333.
(18) Verri, A.; Priori, G.; Spadari, S.; Tondelli, L.; Focher, F. Relaxed enantioselectivity of human mitochondrial thymidine kinase and chemotherapeutic uses of L-nucleoside analogues. *Biochem. J.* **1997**, *328*, 317−320.

(19) Sabini, E.; Hazra, S.; Konrad, M.; Burley, S. K.; Lavie, A. Structural basis for activation of the therapeutic L-nucleoside analogs 3TC and troxacitabine by human deoxycytidine kinase. *Nucleic Acids Res.* **2007**, *35*, 186−192.
(20) Sabini, E.; Ort, S.; Monnerjahn, C.; Konrad, M.; Lavie, A. Structure of human dCK suggests strategies to improve anticancer and antiviral therapy. *Nat. Struct. Biol.* **2003**, *10*, 513−519.
(21) Mahmoudian, M.; Baines, B. S.; Drake, C. S.; Hale, R. S.; Jones, P.; Piercey, J. E.; Montgomery, D. S.; Purvis, I. J.; Storer, R.; Dawson, M. J. Enzymatic production of optically pure (2′*R*-*cis*)-2′-deoxy-3′-thiacytidine (3TC, lamivudine): a potent anti-HIV agent. *Enzyme Microb. Technol.* **1993**, *15*, 749−755.
(22) Wang, J.; Choudhury, D.; Chattopadhyaya, J.; Eriksson, S. Stereoisomeric selectivity of human deoxyribonucleoside kinases. *Biochemistry* **1999**, *38*, 16993−16999.
(23) Zhang, Y.; Secrist, J. A., 3rd; Ealick, S. E. The structure of human deoxycytidine kinase in complex with clofarabine reveals key interactions for prodrug activation. *Acta. Crystallogr., Sect. D: Biol. Crystallogr.* **2006**, *62*, 133−139.
(24) Kabsch, W. Automatic processing of rotation diffraction data from crystals of initially unknown symmetry and cell constants. *J. Appl. Crystallogr.* **1993**, *26*, 795−800.
(25) Vagin, A.; Teplyakov, A. MOLREP: an automated program for molecular replacement. *J. Appl. Crystallogr.* **1997**, *30*, 1022−1025.
(26) Murshudov, G. N.; Vagin, A. A.; Dodson, E. J. Refinement of macromolecular structures by the maximum likelihood method. *Acta Crystallogr.* **1997**, *D53*, 240−255.
(27) Brünger, A. T.; Adams, P. D.; Clore, G. M.; Delano, W. L.; Gros, P.; Grosse-Kunstleve, R. W.; Jiang, J.-S.; Kuszewskli, J.; Nilges, N.; Read, R. J.; Rice, L. M.; Simonson, T.; Warren, G. L. Crystallography and NMR system (CNS): a new software system for macromolecular structure determination. *Acta Crystallogr* **1998**, *D54*, 905−921.
(28) Jones, T. A.; Zhou, J. Y.; Cowan, S. W.; Kjeldgaard, M. Improved methods for building protein models in electron density maps and the location of errors in these models. *Acta Crystallogr.* **1991**, *A47*, 110−119.
(29) Agarwal, K. C.; Miech, R. P.; Parks, R. E., Jr. Guanylate kinases from human erythrocytes, hog brain, and rat liver. *Methods Enzymol.* **1978**, 483−490.

JM0700215